Temperature Dependence of the HO_2 + ClO Reaction. 2. Reaction Kinetics Using the Discharge-Flow Resonance-Fluorescence Technique

Kevin M. Hickson,† Leon F. Keyser, and Stanley P. Sander*

NASA/Jet Propulsion Laboratory, California Institute of Technology, Pasadena, California 91109

Received: December 27, 2006; In Final Form: March 24, 2007

The total rate coefficient, k_3, for the reaction $HO_2 + ClO \rightarrow$ products has been determined over the temperature range of 220−336 K at a total pressure of approximately 1.5 Torr of helium using the discharge-flow resonance-fluorescence technique. Pseudo-first-order conditions were used with both ClO and HO_2 as excess reagents using four different combinations of precursor molecules. HO_2 molecules were formed by using either the termolecular association of H atoms in an excess of O_2 or via the reaction of F atoms with an excess of H_2O_2. ClO molecules were formed by using the reaction of Cl atoms with an excess of O_3 or via the reaction of Cl atoms with Cl_2O. Neither HO_2 nor ClO were directly observed during the course of the experiments, but these species were converted to OH or Cl radicals, respectively, via reaction with NO prior to their observation. OH fluorescence was observed at 308 nm, whereas Cl fluorescence was observed at approximately 138 nm. Numerical simulations show that under the experimental conditions used secondary reactions did not interfere with the measurements; however, some HO_2 was lost on conversion to OH for experiments in excess HO_2. These results were corrected to compensate for the simulated loss. At 296 K, the rate coefficient was determined to be $(6.4 \pm 1.6) \times 10^{-12}$ cm^3 molecule^{-1} s^{-1}. The temperature dependence expressed in Arrhenius form is $(1.75 \pm 0.52) \times 10^{-12} \exp[(368 \pm 78)/T]$ cm^3 molecule^{-1} s^{-1}. The Arrhenius expression is derived from a fit weighted by the reciprocal of the measurement errors of the individual data points. The uncertainties are cited at the level of two standard deviations and contain contributions from statistical errors from the data analysis in addition to estimates of the systematic experimental errors and possible errors from the applied model correction.

Introduction

The most recent assessment of stratospheric ozone depletion[1] concluded that the current chlorine content of the stratosphere has temporarily stabilized at 3.5 ppbv in response to the production regulations on ozone depleting substances in the Montreal Protocol and its amendments. It has been demonstrated that these elevated levels are almost entirely of anthropogenic origin from studies that indicate that the preindustrial mixing ratio of stratospheric Cl_y was about 0.5 ppbv.[2] The enhancement of Cl_y correlates well with observed ozone loss events in the polar stratosphere[3] in addition to the observed negative trend in midlatitude stratospheric ozone concentrations.[4] Most current two-dimensional models underestimate this observation in the midlatitude lower stratosphere, although coupling of chemical and dynamical processes adds to the model uncertainties. In this region of the atmosphere, the dominant catalytic ozone loss mechanism as proposed by Solomon et al.[5] is thought to involve HO_x and ClO_x radical reactions:[6]

$$OH + O_3 \rightarrow HO_2 + O_2 \quad (1)$$

$$k_1(298\ \text{K}) = 7.3 \times 10^{-14}\ \text{cm}^3\ \text{molecule}^{-1}\ \text{s}^{-1}$$

$$Cl + O_3 \rightarrow ClO + O_2 \quad (2)$$

$$k_2(298\ \text{K}) = 1.2 \times 10^{-11}\ \text{cm}^3\ \text{molecule}^{-1}\ \text{s}^{-1}$$

$$HO_2 + ClO \rightarrow HOCl + O_2 \quad (3a)$$

$$k_3(298\ \text{K}) = 5.6 \times 10^{-12}\ \text{cm}^3\ \text{molecule}^{-1}\ \text{s}^{-1}$$

$$HOCl + h\nu \rightarrow Cl + OH \quad (4)$$

$$\text{Net:}\quad 2O_3 \rightarrow 3O_2 \quad (5)$$

HOCl is readily photolyzed by reaction 4 at wavelengths shorter than 420 nm to regenerate Cl and OH radicals. This cycle is thought to be responsible for as much as 30% of the halogen-induced loss of O_3, for which reaction 3a is the rate-determining step.[7] A potential complication to the above mechanism is the existence of another exothermic reaction channel for reaction 3, namely,

$$HO_2 + ClO \rightarrow HCl + O_3 \quad (3b)$$

which would mitigate against ozone loss by partitioning a proportion of the photolabile HOCl into HCl.

There have been four previous studies of the kinetics of reaction 3 at 298 K alone.[8−11] Additionally, three further determinations of the temperature dependence of the rate coefficient[12−14] have been published. All of the studies with data at room temperature report values for k_3 which range from $(3.8-8.3) \times 10^{-12}$ cm^3 molecule^{-1} s^{-1}, the lower number reported by Reimann and Kaufman,[8] the upper number from Nickolaisen et al.[13] The agreement between temperature-dependent studies is poor, especially at low temperatures with values of k_3 ranging from $(5.8-13.7) \times 10^{-12}$ cm^3 molecule^{-1} s^{-1} at approximately 220 K and $(5.7-7.6) \times 10^{-12}$ cm^3

* To whom correspondence should be addressed. Fax: (818) 393-5019. E-mail: ssander@jpl.nasa.gov.

† Present address: Institut des Sciences Moléculaires, Université Bordeaux 1, Talence 33405, France.

10.1021/jp0689464 CCC: $37.00
Published on Web 07/27/2007

molecule^{-1} s^{-1} at approximately 340 K. Furthermore, the earliest of these studies by Stimpfle et al.[12] reports a strongly negative temperature dependence with non-Arrhenius behavior below room temperature, potentially indicative of a complex formation mechanism at these temperatures. Conversely, the other two previous studies conclude that reaction 3 has either a weakly negative temperature dependence[13] or no temperature dependence[14] over their range of study. At 298 K, three of the aforementioned studies[10,11,13] were performed at high pressure (>50 Torr) and four studies[8,9,12,14] at low pressure (<10 Torr). The average values of the high- and low-pressure determinations are (6.5 ± 1.2) and (5.1 ± 1.5) × 10^{-12} cm^3 molecule^{-1} s^{-1}, respectively, as given by a recent evaluation.[6] Although these values lie within the combined uncertainties, the discrepancy might indicate that either secondary reactions could be playing a role in the high- or low-pressure experiments or a small pressure-dependent component to the rate coefficient could exist. In addition to the experimental work, there have been 10 previous theoretical studies[13,15−23] of the ClO + HO_2 reaction or of the potential energy surfaces of the reaction coordinate and the likely intermediates, although until recently the general consensus of these studies was also relatively poor. The results of these theoretical works will be discussed in more detail later in this paper.

In this study, the discharge-flow resonance-fluorescence technique has been used to determine the total rate coefficient k_3 for the HO_2 + ClO reaction over the temperature range of 220−336 K. Specifically, kinetic data have been recorded by monitoring the kinetics of both ClO and HO_2 in the presence of an excess of the other radical species at a total pressure of approximately 1.5 Torr. Efforts were made to eliminate the influence of secondary reactions on the primary process under investigation through the use of several different combinations of radical precursors over a range of temperatures. Furthermore, model calculations were used to quantify the level of possible interference from secondary chemistry for all of the different precursor combinations.

Experimental Section

The flow system used in the present study is essentially that described in a recent paper in detail with a few minor modifications.[24]

Reactor. The main reactor was constructed from Pyrex with an internal diameter of 5.04 cm and was 62 cm in length. The downstream end of the reactor was connected to an octagonal stainless steel resonance-fluorescence cell. The gas pressure was measured via a 10 Torr capacitance manometer (MKS) which was attached to the system between the resonance-fluorescence cell and the reactor. Attached to the upstream end of the reactor were connections to either a fixed HO_2 source and a moveable inlet for the addition of ClO radicals or a moveable HO_2 inlet and a fixed ClO source depending upon the desired method of synthesis for each of the reactants. These sources are described in more detail below. The inner surface of the reaction vessel and the inner and outer surfaces of the moveable inlet and other prereactors attached to the system were coated with halocarbon wax (series 15-00, Halocarbon Corp.) to minimize heterogeneous radical loss. The carrier gas used in all experiments was helium, giving rise to total flows of approximately 2500−2800 sccm (std atm cm^3 min^{-1}), which allowed total flow velocities ranging from 890 to 1400 cm s^{-1}. Measurements were made at temperatures ranging from 220 to 336 K. The flow system was evacuated by a 60 L s^{-1} rotary pump (Edwards E2M175), and a throttling valve was used to maintain the pressure at approximately 1.5 Torr. Temperatures in the reaction zone were maintained to within ±2 K using a temperature-controlled bath (Neslab, ULT-80DD or RTE-100) that circulated a given fluid (methanol or water) through the external jacket of the reactor. Two thermocouples (type E, chromel−constantan) were used to monitor the fluid temperature inside the jacket, one at either end of the reaction vessel.

HO_2 Sources. HO_2 was generated by two different methods during the course of this study. The first method, to produce a low concentration of HO_2 radicals (~5 × 10^{10} molecule cm^{-3}) for most of the experiments in excess ClO, utilized the termolecular reaction[25]

$$H + O_2 + M \rightarrow HO_2 + M \qquad (6)$$

$$k_6(300\ \text{K}) = 1.6 \times 10^{-32}\ \text{cm}^6\ \text{molecule}^{-2}\ \text{s}^{-1}$$

with M being the carrier gas He. H atoms were produced in a 2.45 GHz discharge (60 W) of a dilute mixture of H_2/He in a quartz tube. Total flow rates of He through the discharge were approximately 1300 sccm. The output of the discharge was mixed with a flow of approximately 550 sccm of O_2 in a prereactor coated with halocarbon wax to minimize radical losses. This flow corresponded to concentrations of O_2 in the flow tube in the range of (0.9−1.3) × 10^{16} molecule cm^{-3}. This region, 19 cm long with an internal cross section of 2.5 cm^2, was attached to a fixed side port upstream of the main reactor and was maintained at a pressure of approximately 10 Torr in order to drive the three-body formation of HO_2 through reaction 6. Flow velocities in this prereactor were calculated to be of the order of 1100 cm s^{-1} giving a residence time of approximately 19 ms. Using k_6 = 5.7 × 10^{-32} cm^6 molecule^{-2} s^{-1},[25] we calculate that the H + O_2 reaction was sufficiently fast to prevent any H atoms from entering the main reaction vessel. By this method, HO_2 concentrations as high as 7.0 × 10^{10} molecule cm^{-3} could be produced in the flow system. This method was not suitable for generating high concentrations of HO_2.

The second method, to produce a range of concentrations of HO_2 radicals ((0.1−4.0) × 10^{12} molecule cm^{-3}) for all of the experiments in excess HO_2 and for a series of experiments in excess ClO, utilized the reaction[27]

$$F + H_2O_2 \rightarrow HF + HO_2 \qquad (7)$$

$$k_7(300\ \text{K}) = 5.0 \times 10^{-11}\ \text{cm}^3\ \text{molecule}^{-1}\ \text{s}^{-1}$$

F atoms were generated using a 2.45 GHz discharge (20 W) of a dilute mixture of F_2/He in an alumina tube to improve the F_2 dissociation efficiency. The F atoms were subsequently flowed into the moveable inlet at the upstream end of the reaction vessel through an inner injector. H_2O_2 was contained in a temperature-controlled vessel held at temperatures less than 296 K to prevent H_2O_2 condensation further downstream. A small flow of He was bubbled through the H_2O_2 to carry the vapor into the outer injector of the moveable inlet. The pressure and the temperature within the vessel were monitored to allow the calculation of the H_2O_2 flow into the system. The relative position of the inner injector, which had an internal cross section of 0.2 cm^2, could be altered so that it was possible to vary the reaction time between F + H_2O_2 to ensure that no F atoms entered the main reactor. The moveable inlet itself was 180 cm long with an internal cross section of 1.3 cm^2. The total flow through the moveable inlet was approximately 900 sccm so that flow velocities ranging from 4000 to 6100 cm s^{-1} within the inlet were routinely used. All surfaces within the inlet were coated

with halocarbon wax. H_2O_2 was purified prior to use by pumping and also by bubbling He through it to remove much of the H_2O impurity. The H_2O_2 purity was estimated to be approximately 96 wt % based on earlier measurements[24] under similar experimental conditions.

HO_2 Detection. HO_2 was not directly detected in these experiments. Instead, HO_2 was converted to OH by adding a large excess of NO ($(2.0-4.2) \times 10^{14}$ molecule cm^{-3}) to the flow approximately 5 ms upstream from the resonance cell via the reaction[6]

$$HO_2 + NO \rightarrow OH + NO_2 \qquad (8)$$

$$k_8(298\ K) = 8.1 \times 10^{-12}\ cm^3\ molecule^{-1}\ s^{-1}$$

NO was purified prior to use by passing it through a molecular sieve held at 195 K to remove any potential NO_2 impurity. The OH radicals generated by this titration were subsequently detected by resonance fluorescence. A quartz resonance lamp operated at a microwave power of 65 W was used to excite the incident radiation. A stream of helium saturated with water vapor was flowed through the lamp at a pressure of approximately 1.0 Torr. The light was baffled and collimated prior to entering the resonance cell using a series of concentric rings. Wood's horns were placed opposite the lamp and detection system in order to minimize the detection of scattered light. The resultant hydroxyl radical fluorescence produced in the illuminated portion of the cell was collected perpendicular to the incident radiation after further baffling with an arrangement of rings similar to those on the lamp side. The fluorescence was observed at 308 nm in the (0, 0) band of the OH ($A^2\Sigma^+ - X^2\Pi$) system via an interference filter (Corion 3100-1) and a UV-sensitive photomultiplier tube (EMR 510E). The output of the PMT was then processed using an amplifier−discriminator (Ortec 9302) and counter−timer system (Stanford Research Systems SR400) which were interfaced to a computer for data acquisition and analysis. The interference filter used had a transmission of 17% at 308 nm; it was placed between the PMT and a Suprasil quartz window which formed a vacuum seal to the flow system. As such, the filter was never in contact with any of the reagents used in the experiments. Typically, photons incident on the PMT were integrated over a 10 s period and then averaged over five iterations. During the experimental runs, background fluorescence signals were recorded with the NO flow through the fixed inlet switched off. During the conversion of HO_2 to OH, there was a possibility of radical loss through the reactions[6,26]

$$OH + HO_2 \rightarrow H_2O + O_2 \qquad (9)$$

$$k_9(298\ K) = 1.1 \times 10^{-10}\ cm^3\ molecule^{-1}\ s^{-1}$$

$$OH + OH \rightarrow H_2O + O \qquad (10)$$

$$k_{10}(298\ K) = 1.8 \times 10^{-12}\ cm^3\ molecule^{-1}\ s^{-1}$$

$$OH + NO + He \rightarrow HONO + He \qquad (11)$$

$$k_{11}(300\ K) = 3.3 \times 10^{-31}\ cm^6\ molecule^{-2}\ s^{-1}$$

In order to estimate the magnitude of radical loss, the HO_2 to OH conversion was simulated with computer models. The conversion losses were subsequently incorporated into the HO_2 concentration measurements. These corrections ranged from 10% to 25% with an average value of 18% when HO_2 was used as the excess reagent. Concentrations of excess HO_2 were calculated from the OH fluorescence intensities when measured at an intermediate reaction time. This concentration represented an average of the HO_2 concentrations at the minimum and maximum reaction times due to the heterogeneous loss of HO_2 in addition to its gas-phase self-reaction.[6]

$$HO_2 + HO_2 \rightarrow H_2O_2 + O_2 \qquad (12)$$

$$k_{12}(298\ K) = 1.5 \times 10^{-12}\ cm^3\ molecule^{-1}\ s^{-1}$$

OH Calibration. In order to accurately determine HO_2 concentrations, in particular for experiments where HO_2 was the excess reagent, it was necessary to know the absolute OH concentrations generated by titration with NO. As such, a calibration of the OH resonance-fluorescence lamp was performed on a daily basis to determine its detection sensitivity. Calibrations were performed under similar flow conditions to those used in the experiments to mimic the experiments as much as possible. The system was calibrated by forming specific amounts of OH radicals from the reaction of a known flow of NO_2 and an excess of H atoms[6]

$$H + NO_2 \rightarrow OH + NO \qquad (13)$$

$$k_{13}(298\ K) = 1.3 \times 10^{-10}\ cm^3\ molecule^{-1}\ s^{-1}$$

H atoms were generated as described above, upstream of the main reactor in a fixed side port. A flow of a known composition of NO_2 (corrected for the $NO_2 \rightleftharpoons N_2O_4$ equilibrium) in helium was added to the main flow through the moveable inlet. Due to the removal of a small fraction of the OH radicals within the flow system via reaction 10 during the calibration, the initial NO_2 concentrations were corrected to reflect this loss. The OH signal intensity was recorded, and then the procedure was repeated for different flows of NO_2. A plot of the corrected NO_2 concentration against signal intensity was linear at all OH concentrations. The gradient of the slope of this plot yielded the OH detector sensitivity, S_{OH}. Calibrations were carried out at each temperature used in the experiments although no temperature dependence of the OH sensitivity was observed. Typically, OH count rates varied from 1.0×10^3 to 7.0×10^4 counts s^{-1}. At a typical lamp sensitivity of 2.5×10^{-8} counts s^{-1}/molecule cm^{-3} these count rates corresponded to OH concentrations ranging from 4×10^{10} to 3×10^{12} molecule cm^{-3}. Typical background signals were near 250 counts s^{-1}, and for the 50 s counting times used, a minimum detectable OH concentration of 1.3×10^8 molecule cm^{-3} at a signal-to-noise ratio of unity could be observed.

HO_2 Wall Losses. The loss of HO_2 radicals in the flow system prior to their conversion to OH needed to be considered. These loss rates were not measured directly in this series of experiments but were taken to be the values determined in a recent study[24] ranging from 3.8 to 7.8 s^{-1} over the range of $226 \leq T \leq 296$ K using the same apparatus.

ClO Sources. ClO radicals were generated by two different methods during the course of this study. The first method utilized the reaction of Cl in the presence of an excess of ozone in a prereactor upstream of the main flow system as in reaction 2.

Cl atoms were produced using a 2.45 GHz discharge at 60 W of a dilute mixture of approximately 550 sccm of Cl_2/He in a Suprasil quartz tube. Cl_2 flows into the reactor ranged from 2.6×10^{-3} to 0.4 sccm. The walls of the tube were coated with phosphoric acid immediately downstream of the discharge to minimize the loss of Cl though heterogeneous recombination. The Cl atoms produced were subsequently passed into a fixed 5.0 cm diameter prereactor. Ozone was formed by passing O_2 through a high-voltage discharge ozonizer (Welsbach model

T816). The effluent gas (O_2/O_3) from the ozonizer was subsequently added to the prereactor, thereby generating ClO radicals through reaction 2. The resultant gas mixture was then either passed through the moveable inlet (for experiments in excess ClO) or through a fixed side port (for experiments in excess HO_2) into the main flow system. O_3 concentrations within the ClO source reactor ranged from 2.3×10^{14} to 2.8×10^{15} molecule cm^{-3}. Ozone concentrations were not measured within the flow tube but were calculated to be in the range from $(2-5) \times 10^{13}$ molecule cm^{-3}. This assumed that no depletion of the initial ozone occurred via reaction with Cl or that no ozone was lost heterogeneously or otherwise. As such, these values are an upper limit for $[O_3]$. Every effort was taken to minimize the concentration of ozone allowed to enter the flow tube to prevent secondary reactions, although sufficient ozone was maintained to ensure that no Cl atoms entered the flow tube from the ClO source. Otherwise the reaction[6]

$$Cl + HO_2 \rightarrow HCl + O_2 \quad (14a)$$

$$k_{14a}(298\ K) = 3.2 \times 10^{-11}\ cm^3\ molecule^{-1}\ s^{-1}$$

$$\rightarrow OH + ClO \quad (14b)$$

$$k_{14b}(298\ K) = 9.1 \times 10^{-12}\ cm^3\ molecule^{-1}\ s^{-1}$$

might rapidly remove HO_2 radicals, a considerable problem for experiments in excess ClO which rely on accurately measuring the HO_2 decay rates. No residual Cl atoms were observed in the reactor in any of the experiments.

When ClO was passed into the main flow system through the fixed side port the total pressure in the source was approximately 2.5 Torr. At the total flow rate of 600 sccm, the flow velocity in the source was approximately 170 cm s^{-1}. The reaction length was approximately 18 cm which gave a reaction time of greater than 100 ms. Using $k_2 = 1.2 \times 10^{-11}$ cm^3 $molecule^{-1}$ s^{-1}, it is clear that reaction was complete within the source before any unreacted Cl atoms could reach the flow tube. Furthermore, when ClO was passed into the main flow system via the moveable inlet, the pressure in the source increased to approximately 15 Torr. This significantly extended the reaction time in the source. By this method, ClO concentrations within the range of 3×10^{10} to 7×10^{12} molecule cm^{-3} could be produced within the flow tube.

The second method used to produce an excess of ClO radicals within the flow system utilized the reaction[6]

$$Cl + Cl_2O \rightarrow ClO + Cl_2 \quad (15)$$

$$k_{15}(298\ K) = 9.6 \times 10^{-11}\ cm^3\ molecule^{-1}\ s^{-1}$$

Cl_2O was synthesized in separate experiments by passing Cl_2 over dehydrated yellow mercuric(II) oxide

$$2Cl_2 + HgO \rightarrow Cl_2O + HgCl_2 \quad (16)$$

Cl_2O was trapped at 156 K using an ethanol/liquid nitrogen slush bath. During the experiments, the Cl_2O was held at 195 K using a dry ice/methanol slush, while a flow of approximately 60 sccm of He was bubbled through the liquid Cl_2O and into a side port of the moveable inlet. The major impurity in the Cl_2O was found to be Cl_2 by UV absorption methods; however, the Cl_2 content of the synthesized Cl_2O was found to decrease over time due to its higher vapor pressure at dry ice temperatures (65 Torr vs 7 Torr for Cl_2O).

As described earlier, Cl atoms were produced using a 2.45 GHz discharge at 60 W of a dilute mixture of approximately 600 sccm of Cl_2/He in a Suprasil quartz tube. These Cl atoms were passed directly into the moveable inlet where they were mixed with the flow of He carrying Cl_2O vapor. This gave rise to concentrations of Cl_2O within the injector from $(5.0-7.5) \times 10^{13}$ molecule cm^{-3}. Cl_2 flows into the inlet ranged from 3×10^{-2} to 0.45 sccm. Residence times within the moveable inlet ranged from 60−80 ms which indicate that reaction 15 was complete before any Cl atoms could enter the main flow system. Furthermore, simulations suggest that a significant depletion of Cl_2O occurred within the moveable inlet through reaction 15. This gave rise to concentrations of Cl_2O within the main flow system from $(5-7) \times 10^{12}$ molecule cm^{-3}. As with the $Cl + O_3$ synthesis, every effort was made to minimize the Cl_2O concentration entering the flow system to prevent secondary reactions, although Cl_2O was maintained at a high enough concentration such that no Cl atoms were observed in the flow system.

When added through the moveable inlet, ClO concentrations were measured at intermediate reaction times to account for the removal of a small fraction of the ClO through wall loss and self-reaction in the main reactor[6]

$$ClO + ClO \rightarrow Cl_2 + O_2 \quad (17a)$$

$$k_{17a}(298\ K) = 4.8 \times 10^{-15}\ cm^3\ molecule^{-1}\ s^{-1}$$

$$ClO + ClO \rightarrow 2Cl + O_2 \quad (17b)$$

$$k_{17b}(298\ K) = 8.0 \times 10^{-15}\ cm^3\ molecule^{-1}\ s^{-1}$$

$$ClO + ClO \rightarrow OClO + Cl \quad (17c)$$

$$k_{17c}(298\ K) = 3.5 \times 10^{-15}\ cm^3\ molecule^{-1}\ s^{-1}$$

$$ClO + ClO + He \rightarrow (ClO)_2 + He \quad (18)$$

$$k_{18}(300\ K) = 0.99 \times 10^{-32}\ cm^6\ molecule^{-2}\ s^{-1}$$

Heterogeneous losses of ClO were not measured in these experiments. Previous measurements of this quantity[28,29] have shown that in both coated and uncoated Pyrex reactors with a surface-to-volume ratio of less than 2 cm^{-1} wall loss rates for ClO were in the range of $0.1-2$ s^{-1} at temperatures as low as 183 K. Using a wall loss rate of 1 s^{-1} as an average value, we estimate that the percentage of ClO lost due to surface reaction is less than 3%, whereas the loss of ClO through reactions 17a−17c is less than 1% at 296 K when ClO is flowed through the moveable inlet. When ClO is flowed through the fixed side port, the estimated percentage of ClO lost heterogeneously rises to 8%, whereas the loss of ClO through reactions 17a−17c is negligible. The rate coefficient value given for reaction 18 is for N_2 as the third body; therefore, the value in He is expected to be 2−3 times smaller. As such, the formation of $(ClO)_2$ is negligible under all conditions used, even in the moveable inlet itself where the ClO concentration is elevated prior to dilution by the main flow.

ClO Detection. ClO was not directly detected during these experiments. Instead, ClO was initially converted to Cl by adding a large excess of NO ($(2.0-4.2) \times 10^{14}$ molecule cm^{-3})

to the flow approximately 5 ms upstream from the resonance cell via the reaction[6]

$$ClO + NO \rightarrow Cl + NO_2 \qquad (19)$$

$$k_{19}(298\ K) = 1.7 \times 10^{-11}\ cm^3\ molecule^{-1}\ s^{-1}$$

As with the conversion of HO_2 to OH, NO was purified prior to use by passing it through a molecular sieve held at 195 K to remove any potential NO_2 impurity.

Chlorine atoms were observed via resonance fluorescence, in an octagonal detection cell downstream from the temperature-controlled portion of the flow system. A 60 W microwave discharge of a mixture of approximately 0.13% Cl_2 in He held at 1.5 Torr was used to produce chlorine atom emission. The light emitted from the lamp was subsequently passed through a CaF_2 window which formed a seal to the flow system. Before entering the resonance cell, the incident radiation was collimated using a series of concentric rings to minimize background scatter. The chlorine atoms within the illuminated portion of the gas flow were excited and subsequently emitted fluorescence on-resonance with the exciting radiation, mainly in the $(4s^13p^4)^4P_{3/2} \rightarrow (3p^5)^2P_{3/2}$ transition at 137.96 nm. The fluorescence was observed perpendicular to the incident radiation using a channel photomultiplier (CPM) (Perkin-Elmer 1911P) which was sensitive to wavelengths between 120 and 200 nm. A 1 mm thick BaF_2 window immediately in front of the CPM was used as a cut-on filter to eliminate possible interferences from oxygen and hydrogen atom emission. It was thought that this might potentially result from the microwave discharge of impurities in some of the buffer gas flows although no emission was ever observed from these sources during the experiments. A second series of baffles was used in front of the BaF_2 window, and Wood's horns were placed opposite the lamp and CPM in order to reduce further the detection of scattered light. The CPM output signal was passed to a photon counting system (Stanford Research Systems SR400) where, typically, signals were integrated for 10 s and averaged over five iterations. During the experimental runs, background fluorescence signals were recorded with the NO flow switched off so that no chlorine atoms formed by reaction 19 were observed.

Cl Calibration. In order to accurately determine ClO radical concentrations, in particular for experiments where ClO was used as the excess reagent, it was necessary to calibrate the chlorine atom concentrations on a daily basis. The sensitivity of the detection system to Cl atom concentrations in the flow cell was determined by generating a known concentration of Cl atoms via the reaction of excess F atoms with Cl_2[27]

$$F + Cl_2 \rightarrow Cl + FCl \qquad (20)$$

$$k_{20}(298\ K) = 1.6 \times 10^{-10}\ cm^3\ molecule^{-1}\ s^{-1}$$

F atoms were produced in a microwave discharge of a 1% mixture of F_2 in helium in a fixed port upstream of the main reactor. An uncoated 1 cm i.d. alumina tube was used in the microwave source, which was operated at 20 W. Typical flow rates through the discharge were on the order of 600 sccm. Background signals, which consisted of scattered light and light from secondary sources of Cl atoms, were determined by simply turning off the Cl_2 flow with all other flows on. Calibrations were performed under similar flow conditions to those used in the experiments. It was discovered that when O_2 was added to the system for the generation of HO_2 radicals by reaction 6 and also from the effluent of the ozonizer, the sensitivity to Cl was reduced by a significant amount due to absorption of lamp light. As such, all calibrations were performed with O_2 concentrations identical to those used in experimental runs. Typical detection sensitivities were found to be in the region of 1.7×10^{-6} counts s^{-1}/atoms cm^{-3} with background signals at about 2500 counts s^{-1} for Cl atom concentrations less than approximately 9×10^{12} atoms cm^{-3}. For a 50 s counting time, this was equivalent to a minimum detectable Cl atom concentration of 6×10^6 atoms cm^{-3} at a signal-to-noise ratio of unity. For higher concentrations, such as when the experiments were performed in excess ClO, the Cl atom sensitivity was found to be nonlinear. Under these conditions, a polynomial function was fitted to the measured chlorine atom intensities obtained. The fitting function was then used to calculate experimental Cl atom concentrations from the observed intensities. The calibrations were performed at the same temperatures and pressures as the experiments themselves although no temperature dependence of the Cl atom signals was observed.

Calibrations. The mass flow controllers and meters (MKS and Hastings) used during the course of the experiments were calibrated for the particular gas mixture to be flowed using a pressure drop/rise at constant volume method. Factory-calibrated capacitance manometers (MKS) were used to calibrate the pressure gauges on the system. The thermocouples used to monitor the cell temperature were calibrated at 273 and 195 K using ice/water and CO_2(s)/ethanol mixtures, respectively. The internal temperature of the flow tube was measured at several positions using a thermocouple probe in place of the usual moveable inlet. At room temperature (296 K) and above, the probe temperature was within 0.1 K of the jacket thermocouple temperatures. At low temperatures the probe temperature and jacket thermocouple temperatures were within 1 K, the probe thermocouple reading the lower of the two. The reported temperatures are those measured using the probe thermocouple.

Corrections. The observed pseudo-first-order rate coefficients were corrected for axial and radial diffusion. The diffusion coefficients for ClO in He and HO_2 in He were estimated to be $0.0252T^{1.72}$ Torr $cm^2\ s^{-1}$ and $0.0332T^{1.71}$ Torr $cm^2\ s^{-1}$ from calculations of the diffusion coefficients of similar relative molecular mass species in He.[30] These gave rise to corrections to the rate coefficients of between 1.1% and 7.8%. No corrections were made for the viscous pressure drop between the reaction zone and the pressure measurement port because earlier observations using the present reactor showed that the corrections were less than 0.5%.

Reagents. High-purity chemicals were used in order to minimize the introduction of impurities into the flow. Research grade He (99.9999%) was further purified prior to use by flowing through a molecular sieve (Linde 3A) trap held at 77 K. Furthermore, research grade O_2 (99.999%), research grade Cl_2 (99.999%), research grade H_2 (99.9999%), CP grade NO (99%) which was further purified prior to use by flowing through a molecular sieve (Linde 3A) trap held at 195 K, and 1% mixtures of F_2 in He were also used. H_2O_2 (90%) which was further purified by pumping prior to use, Cl_2O which was synthesized in separate experiments, and NO_2 which was prepared from NO by adding excess O_2 were all used during the course of the experiments.

Kinetic Results

Different combinations of precursor molecules were used to produce the reagent species in four separate sets of experiments as described earlier. Three of these were performed in an excess of ClO, and one set of experiments was performed in an excess of HO_2. These conditions are summarized in Table 1.

TABLE 1: Summary of the Main Experimental Conditions

precursor combination	excess reagent	[excess]/ 10^{12}	location of excess reagent	minor reagent	[minor]/ 10^{10}	location of minor reagent
$Cl + O_3/H + O_2 + M$	ClO	0.5−6.0[a]	moveable injector	HO_2	<5.0[a]	side arm
$Cl + Cl_2O/H + O_2 + M$	ClO	0.4−10	moveable injector	HO_2	<5.0	side arm
$Cl + O_3/F + H_2O_2$	ClO	0.1−5.0	side arm	HO_2	<10	moveable injector
$Cl + O_3/F + H_2O_2$	HO_2	0.4−3.0	moveable injector	ClO	<3.0	side arm

[a] With units of molecule cm^{-3}.

Excess ClO. *Data Analysis.* Under the conditions where ClO was added as the excess reagent, the loss of HO_2 radicals was well described by a pseudo-first-order decay profile. When ClO was added to system, the loss of HO_2 could be written as

$$-d[HO_2]/dt = k_3[HO_2][ClO] + k_{L,HO2}[HO_2] \quad (21)$$

Here $k_{L,HO2}$ represents the pseudo-first-order loss of HO_2 radicals in the absence of ClO. This was thought to be due to a combination of wall losses and gas-phase reactions such as reaction 12. We convert HO_2 to OH for detection purposes, and as such, reference to OH will be made in lieu of HO_2. The OH resonance-fluorescence signal, I_{OH}, varied linearly with [OH] at the concentrations used in these experiments, i.e., $[OH] = I_{OH}/S_{OH}$, and [ClO] was in large enough excess to be effectively constant. Consequently, it could be written that

$$-d\ln[I_{OH}]/dt = k_3' + k_{L,HO2} \quad (22)$$

where $k_3' = k_3[ClO]$. Values of $k_3' + k_{L,HO2}$ were determined from the slopes of $\ln(I_{OH})$ against reaction length (l) plots by linear least-squares analysis. Under plug flow conditions, the reaction time was subsequently calculated by the relationship $t = l/v$ where v represents the flow velocity. Typical reaction lengths used varied from 5 to 26 cm giving rise to reaction times of between 3.6 and 29 ms.

ClO from Cl + O_3, HO_2 from H + O_2 + M. ClO concentrations used were in the range of 5×10^{11} to 6×10^{12} molecule cm^{-3} with initial HO_2 concentrations ranging from $(4-5) \times 10^{10}$ molecule cm^{-3}. Initial stoichiometric ratios ranged from 10 to 120. O_3 and O_2 concentrations were in the range of $(2-5) \times 10^{13}$ and $(1.0-1.5) \times 10^{16}$ molecule cm^{-3}, respectively. Measurements were made at temperatures ranging from 220 to 336 K and at an approximate total pressure of 1.5 Torr of helium. An example of the resultant second-order plots obtained for this combination of precursor molecules is shown in Figure 1. The lower intercept value of the fit to the data at 220 K compared to the value obtained for 336 K is indicative of the uncertainties in the data. At 220 and 336 K the intercept values are (-1.0 ± 1.4) s^{-1} and (0.7 ± 0.9) s^{-1}, respectively. The measured rate coefficients are summarized in Table 2.

An Arrhenius plot of the data presented in Table 2 for the Cl + O_3/H + O_2 + M precursor combination yields the following expression for $220 \le T \le 336$ K:

$$k_3 = (1.92 \pm 0.92) \times 10^{-12} \exp[(351 \pm 122)/T] \text{ cm}^3 \text{ molecule}^{-1} \text{ s}^{-1} \quad (23)$$

ClO from Cl + Cl_2O, HO_2 from H + O_2 + M. ClO concentrations used were in the range of 3.5×10^{11} to 9.5×10^{12} molecule cm^{-3} with initial HO_2 concentrations ranging from $(4-5) \times 10^{10}$ molecule cm^{-3}. Initial stoichiometric ratios ranged from 7 to 190. Cl_2O concentrations were calculated to be in the range of $(5-8) \times 10^{12}$ molecule cm^{-3}, and O_2 concentrations were in the range of $(0.9-1.3) \times 10^{16}$ molecule cm^{-3}. Measurements were made at temperatures ranging from 230 to 336 K and at an approximate total pressure of 1.5 Torr of helium. A summary of the measured rate coefficients is given in Table 2.

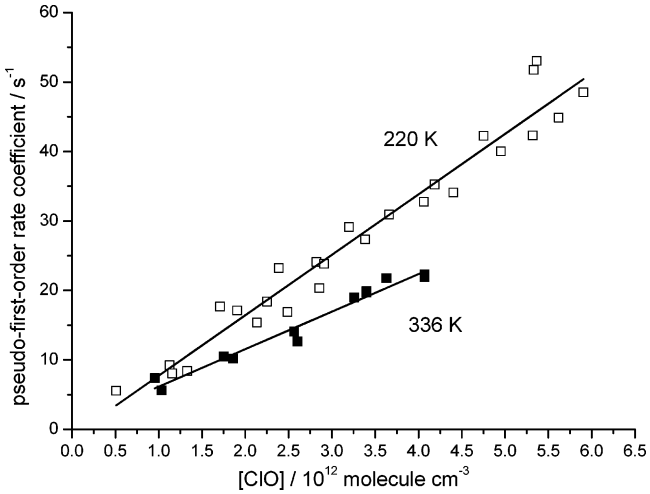

Figure 1. Second-order plots of typical results from the current study. ClO and HO_2 radicals were generated using Cl + O_3 and H + O_2 + M as their respective precursors. □ Experimental data taken at 220 K. ■ Experimental data taken at 336 K. The two lines represent the linear least-squares fits to the respective data sets.

An Arrhenius plot of the data presented in Table 2 for the Cl + Cl_2O/H + O_2 + M precursor combination yields the following expression for $230 \le T \le 336$ K:

$$k_3 = (2.08 \pm 1.14) \times 10^{-12} \exp[(357 \pm 144)/T] \text{ cm}^3 \text{ molecule}^{-1} \text{ s}^{-1} \quad (24)$$

ClO from Cl + O_3, HO_2 from F + H_2O_2. ClO concentrations used were in the range of 1.3×10^{11} to 5.4×10^{12} molecule cm^{-3} with initial HO_2 concentrations approximately $(9-10) \times 10^{10}$ molecule cm^{-3}. Initial stoichiometric ratios ranged from 2 to 68. O_3 and O_2 concentrations were in the range of $(2.2-3.0) \times 10^{13}$ and $(7.0-9.0) \times 10^{14}$ molecule cm^{-3}, respectively. H_2O_2 concentrations were in the range of $(3.5-4.9) \times 10^{12}$ molecule cm^{-3}. Measurements were made at temperatures ranging from 242 to 336 K and at an approximate total pressure of 1.5 Torr of helium. A summary of the measured rate coefficients is given in Table 2.

An Arrhenius plot of the data presented in Table 2 for the Cl + O_3/F + H_2O_2 precursor combination yields the following expression for $242 \le T \le 336$ K:

$$k_3 = (1.74 \pm 1.18) \times 10^{-12} \exp[(372 \pm 188)/T] \text{ cm}^3 \text{ molecule}^{-1} \text{ s}^{-1} \quad (25)$$

Excess HO_2. Concentrations of HO_2 were in the range of 4.1×10^{11} to 2.7×10^{12} molecule cm^{-3} with initial ClO radical concentrations of approximately 3×10^{10} molecule cm^{-3}. Initial stoichiometric ratios ranged from 14 to 90. H_2O_2 concentrations were estimated to be between 0.8×10^{13} and 1.0×10^{13} molecule cm^{-3}. O_3 concentrations were estimated to be in the

TABLE 2: Measured Values for k_3[a]

T/K	precursor combination[b]	no. of measurements	[ClO]/[HO_2][c]	k_3[d]
336	**Cl** + **O_3**/H + O_2 + M	12	0.9−4.1	5.40 ± 0.69[e,f]
336	**Cl** + **Cl_2O**/H + O_2 + M	9	0.8−6.6	5.68 ± 1.33
336	**Cl** + **O_3**/F + H_2O_2	14	0.3−4.1	5.42 ± 0.80
336	Cl + O_3/**F** + **H_2O_2**	12	0.4−2.4	5.12 ± 0.76[g,h]
316	**Cl** + **O_3**/H + O_2 + M	10	0.8−4.3	6.06 ± 1.07
316	**Cl** + **Cl_2O**/H + O_2 + M	12	0.8−6.5	6.09 ± 0.70
316	**Cl** + **O_3**/F + H_2O_2	8	0.4−4.2	5.48 ± 0.40
296	**Cl** + **O_3**/H + O_2 + M	18	1.2−4.5	6.18 ± 0.68
296	**Cl** + **Cl_2O**/H + O_2 + M	22	1.0−7.9	7.05 ± 0.96
296	**Cl** + **O_3**/F + H_2O_2	13	0.1−2.9	6.53 ± 0.71
296	Cl + O_3/**F** + **H_2O_2**	8	0.4−2.7	5.88 ± 0.86[g,h]
276	**Cl** + **O_3**/H + O_2 + M	23	1.3−5.5	6.57 ± 0.64
276	**Cl** + **Cl_2O**/H + O_2 + M	18	1.1−9.4	8.04 ± 0.86
276	**Cl** + **O_3**/F + H_2O_2	12	0.4−4.8	6.42 ± 0.48
276	Cl + O_3/**F** + **H_2O_2**	11	0.4−2.4	6.31 ± 0.70[g,h]
256	**Cl** + **O_3**/H + O_2 + M	15	1.4−5.1	7.73 ± 1.15
256	**Cl** + **Cl_2O**/H + O_2 + M	30	1.0−9.5	8.76 ± 0.64
256	**Cl** + **O_3**/F + H_2O_2	12	0.5−5.4	7.40 ± 0.57
256	Cl + O_3/**F** + **H_2O_2**	11	0.6−2.2	6.66 ± 0.86[g,h]
242	**Cl** + **O_3**/H + O_2 + M	18	1.3−5.6	8.12 ± 1.39
242	**Cl** + **Cl_2O**/H + O_2 + M	12	0.6−8.7	9.31 ± 0.82
242	**Cl** + **O_3**/F + H_2O_2	15	0.5−5.4	8.27 ± 1.10
230	**Cl** + **O_3**/H + O_2 + M	24	0.8−6.0	10.00 ± 1.08
230	**Cl** + **Cl_2O**/H + O_2 + M	22	0.3−8.0	9.21 ± 0.92
220	**Cl** + **O_3**/H + O_2 + M	26	0.5−5.6	8.70 ± 0.92

[a] Corrected for axial and radial diffusion. [b] The precursor combination used for excess reagent production is highlighted. [c] Excess reagent concentration units 10^{12} molecule cm^{-3}. [d] Units 10^{-12} cm^3 $molecule^{-1}$ s^{-1}. [e] Errors are cited at the level of two standard deviations and include a contribution from estimated systematic errors. [f] From plots of k_3[ClO] versus [ClO]. [g] From plots of k_3[HO_2] versus [HO_2]. [h] Errors are cited at the level of two standard deviations and include contributions from estimated systematic errors and an estimated model correction error.

range of (1.8−2.3) × 10^{13} molecule cm^{-3}. O_2 concentrations were in the range of (5.3−6.9) × 10^{14} molecule cm^{-3}. Measurements were made at temperatures ranging from 256 to 336 K and at an approximate total pressure of 1.5 Torr of helium.

Data Analysis. Under the conditions described above, the loss of ClO radicals was well described by a pseudo-first-order decay profile. When HO_2 was added to system, the loss of ClO could be written as

$$-\mathrm{d[ClO]}/\mathrm{d}t = k_3[\mathrm{HO_2}][\mathrm{ClO}] + k_{\mathrm{L,ClO}}[\mathrm{ClO}] \qquad (26)$$

Here $k_{\mathrm{L,ClO}}$ represents the pseudo-first-order loss of ClO in the absence of HO_2. This was thought to be mainly due to heterogeneous reactions and also secondary gas-phase reactions may have contributed to a small loss as described earlier. As we convert ClO to Cl for detection purposes it is proper to refer to Cl in place of ClO. As the Cl resonance-fluorescence signal, I_{Cl}, varied linearly with [Cl] at the low concentrations used in these experiments, i.e., $[\mathrm{Cl}] = I_{\mathrm{Cl}}/S_{\mathrm{Cl}}$, and [$HO_2$] was in excess, it could be written that

$$-\mathrm{d}\ln[I_{\mathrm{Cl}}]/\mathrm{d}t = k_3' + k_{\mathrm{L,ClO}} \qquad (27)$$

where $k_3' = k_3[\mathrm{HO_2}]$. Values of $k_3' + k_{\mathrm{L,ClO}}$ were determined from the slopes of $\ln(I_{\mathrm{Cl}})$ against reaction length (l) plots by linear least-squares analysis. Under plug flow conditions, the reaction time was subsequently calculated by the relationship $t = l/v$ where v represents the flow velocity. Typical reaction lengths used varied from 5 to 26 cm giving rise to reaction times of between 3.6 and 26.0 ms. A summary of the measured rate coefficients is given in Table 2.

An Arrhenius plot of the data presented in Table 2 for the Cl + O_3/F + H_2O_2 precursor combination for an excess of HO_2 yields the following expression for 256 ≤ T ≤ 336 K:

$$k_3 = (2.24 \pm 2.52) \times 10^{-12} \exp[(283 \pm 318)/T] \ \mathrm{cm^3\ molecule^{-1}\ s^{-1}} \qquad (28)$$

Experiments were limited to temperatures greater than 256 K due to the difficulty of producing HO_2 in excess at low temperatures. Furthermore, these experimentally determined values for an excess of HO_2 in Table 2 have been corrected using the output of a numerical model of the experimental system. The measurement errors given for the excess HO_2 data are obtained from an unweighted linear least-squares analysis, are cited at the level of two standard deviations, and include contributions from the systematic uncertainties. Moreover, these uncertainty estimates also contain a contribution from the possible error in the applied model correction. The model results are discussed later. The uncertainty in the applied model correction was quantified by evaluating current uncertainties in the rate coefficients for the three reactions responsible as given by the most recent evaluation.[6] An Arrhenius plot of the combination of the four experimentally determined data sets yields the following expression:

$$k_3 = (1.75 \pm 0.52) \times 10^{-12} \exp[(368 \pm 78)/T] \ \mathrm{cm^3\ molecule^{-1}\ s^{-1}} \qquad (29)$$

This expression is valid over the range of 220 ≤ T ≤ 336 K and is plotted in Figure 2 alongside the currently available temperature-dependent data for the ClO + HO_2 reaction, inclusive of the current study. The measurement errors for the expressions 23−25 and 28−29 are obtained from a linear least-squares analysis weighted as a function of the reciprocal of the uncertainties for each data point and are cited at the level of two standard deviations.

Discussion

Numerical Modeling and Secondary Chemistry. Computer models were used to check for losses encountered during conversion of both HO_2 to OH and ClO to Cl. Furthermore, these calculations were also used to check for possible interferences from secondary reactions. The simulations were carried out using the CHEMRXN program, which has been validated

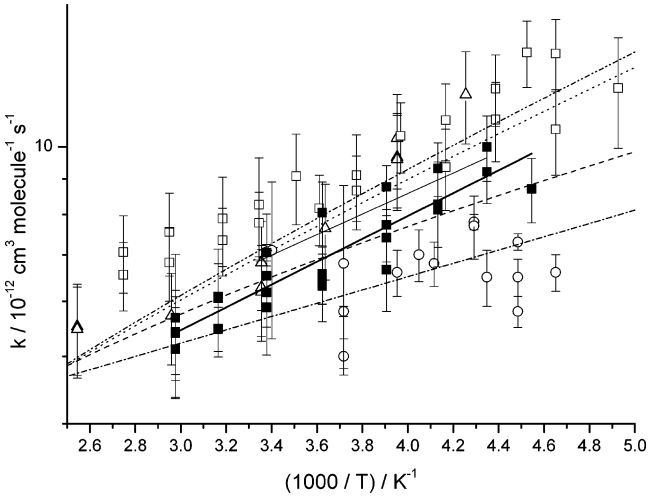

Figure 2. Arrhenius plot of the results from the current study compared to earlier work. Experimental data from △ Stimpfle et al. (ref 12), □ Nickolaisen et al. (ref 13), ○ Knight et al. (ref 14), ■ current study; — fit to current study weighted by the reciprocal of the respective uncertainties for each point; Xu et al. (ref 23) theoretical prediction at (a) − − 1 Torr, (b) · · · 400 Torr, (c) · · — · · 760 Torr; · — · recommendation from Sander et al. (ref 6); — recommendation from Atkinson et al. (ref 32).

versus a standard differential integrator and a stochastic algorithm.[31] The rate coefficients used in the models were taken from three separate compendia: the NASA−JPL Chemical Kinetics Data Evaluation,[6] the NIST Chemical Kinetics Database,[27] and the IUPAC Gas Kinetics Data Evaluation.[32]

Models were used to test for losses of HO_2 and ClO during the HO_2 + NO and ClO + NO titrations for all four of the different experimental systems at 298 K. To imitate the experiments as closely as possible, input concentrations of all radical and nonradical species were entered into the model such that they were representative of the actual experimental flow system values (known or estimated). Then, the model was initially run with no NO present at several different reagent contact times to simulate the different injector positions used in the experiments. The resultant species concentrations from each run were subsequently re-entered into the model for a further 5 ms in the presence of NO to simulate the HO_2 to OH and ClO to Cl titration processes. As we do not observe either of the initial reagents directly, the resulting concentrations of OH and Cl radicals generated by the model were taken to be the equivalent of the experimental observations. As the model is conducted under pseudo-first-order conditions, the natural logarithms of the output minor reagent concentrations were plotted versus time for each of the output excess reagent concentrations. A least-squares fit to the time series was used to generate a pseudo-first-order decay rate, $k_{3(out)}'$, from the slope. The whole process was repeated for many different combinations of initial [ClO] and [HO_2]. The change in k_3' induced by secondary reactions and/or the titration process was then obtained using the following relation: del % = $((k_{3(out)}' - k_{3(in)}')/k_{3(in)}') \times 100$. $k_{3(in)}'$ with units of s^{-1} is the product of the input rate coefficient, $k_{3(in)} = 5.6 \times 10^{-12}$ cm^3 $molecule^{-1}$ s^{-1}, and the concentration of the excess reagent at an intermediate reaction time (to apply a correction for the loss of the excess reagent in the flow system through secondary reactions). Contour plots were subsequently generated for del % at the different output OH and Cl concentrations used in the model.

Excess HO_2 from F + H_2O_2, ClO from Cl + O_3. Input concentrations of HO_2 were in the range of 5×10^{11} to 5×10^{12} molecule cm^{-3}; concentrations of initial ClO were in the range of 3×10^9 to 3×10^{11} molecule cm^{-3}. Initial concentrations of H_2O_2, O_3, and O_2 were also included at the outset of the model run with input values of 9×10^{12}, 2×10^{13}, and 6×10^{14} molecule cm^{-3}, respectively, obtained from estimates of the concentrations within the experimental system. NO was subsequently added to the system at a concentration of 3×10^{14} molecule cm^{-3}. The resultant contour plot calculated using these input values is shown in Figure 3.

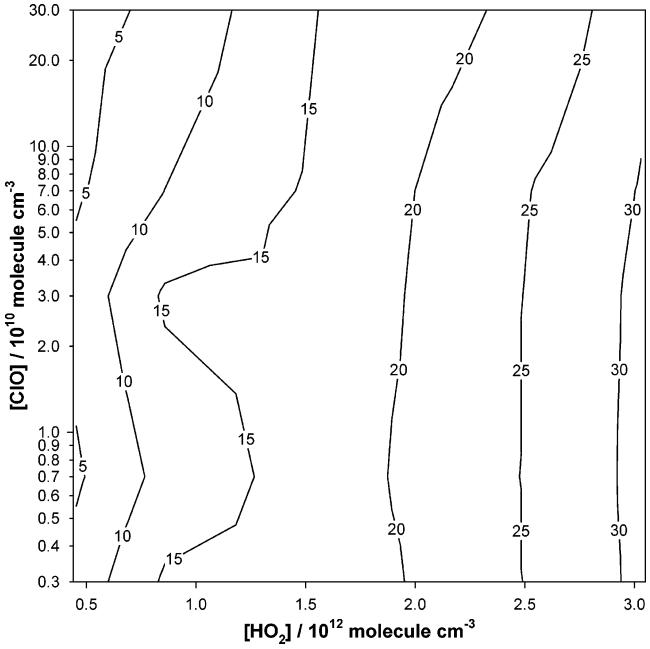

Figure 3. Calculated percent change in k_3' induced by secondary reactions and/or the titration process for a range of HO_2 and ClO concentrations with HO_2 as the excess reagent. Typical [ClO] = 3×10^{10} molecule cm^{-3}. Percentage value reflects the difference between output and input values as given by del % = $((k_{3(out)}' - k_{3(in)}')/k_{3(in)}') \times 100$.

The effect of secondary chemistry and/or problems in the titration process for experiments in excess HO_2 presented in Figure 3 clearly predicts that a significant deviation should occur for the observed range of reagent ([ClO] = 3×10^{10} molecule cm^{-3} and [HO_2] = 4.1×10^{11} to 2.7×10^{12} molecule cm^{-3}) and precursor concentrations. From model sensitivity analyses, approximately 90% of these deviations can be shown to result from three reactions, namely, reactions 9−11, which all occur within the 5 ms titration region of the flow system. It should be noted at this point that the discrepancy arises from a loss of HO_2 prior to its conversion to OH, rather than an error in the observed k_3'. In effect, the observed [HO_2] is lower than the actual [HO_2]. Reaction 9 is a particularly fast process and accounts for over 50% of the total loss of OH and HO_2. As a result of the model calculations, corrections were applied to the experimentally observed HO_2 concentrations for each measured k_3'. The magnitude of the applied correction was determined by cross-referencing the experimentally observed [HO_2] with the calculated contours. As a result, the experimentally observed rate coefficients were seen to decrease by between 24% and 30% after correction. The values presented in Table 2 are the corrected second-order rate coefficients. As this problem arises within the titration region, outside of the temperature-controlled portion of the flow system, it was only necessary to perform these calculations at room temperature. Therefore, the applied corrections were valid for all temperatures investigated.

Excess ClO from Cl + O_3, HO_2 from H + O_2 + M. Input concentrations of ClO were in the range of 5×10^{11} to $8 \times$

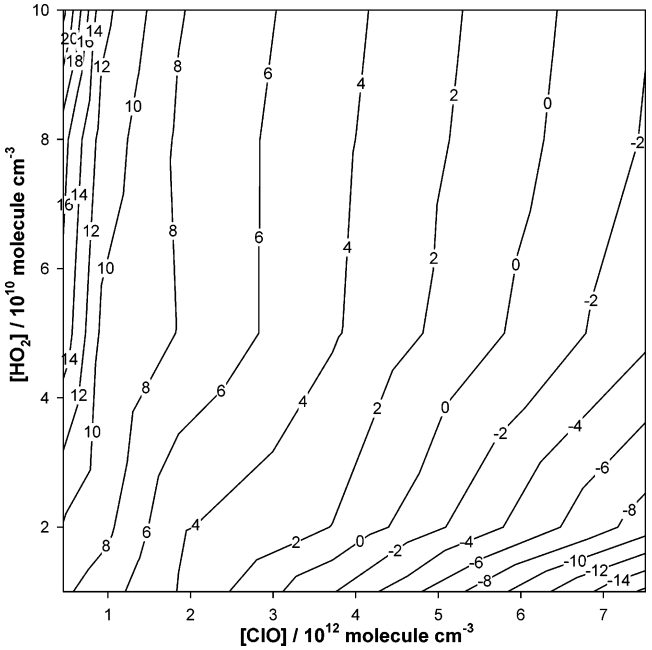

Figure 4. Calculated percent change in k_3' induced by secondary reactions and/or the titration process for a range of HO_2 and ClO concentrations from the precursor combination $H + O_2 + M/Cl + O_3$ with ClO as the excess reagent. Typical $[HO_2] = 5 \times 10^{10}$ molecule cm^{-3}. Percentage value reflects the difference between output and input values as given by del % = $((k_{3(out)}' - k_{3(in)}')/k_{3(in)}') \times 100$.

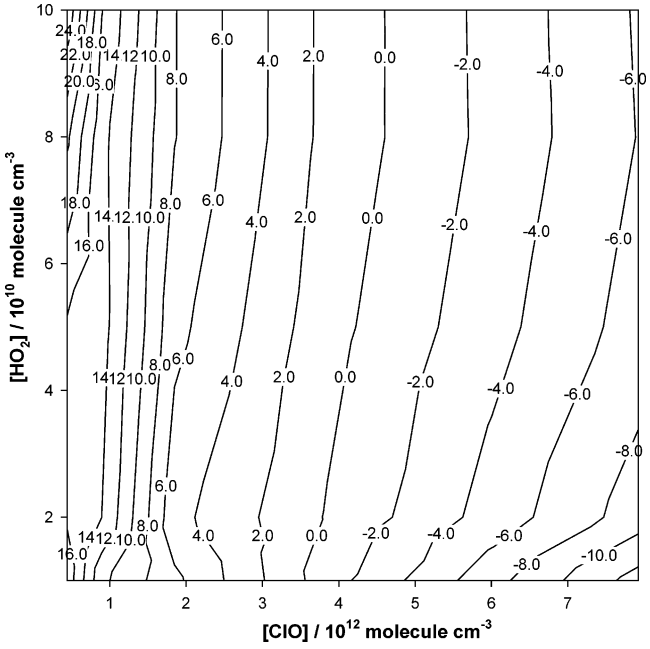

Figure 5. Calculated percent change in k_3' induced by secondary reactions and/or the titration process for a range of HO_2 and ClO concentrations from the precursor combination $H + O_2 + M/Cl + Cl_2O$ with ClO as the excess reagent. Typical $[HO_2] = 5 \times 10^{10}$ molecule cm^{-3}. Percentage value reflects the difference between output and input values as given by del % = $((k_{3(out)}' - k_{3(in)}')/k_{3(in)}') \times 100$.

10^{12} molecule cm^{-3}; concentrations of initial HO_2 were in the range of 1×10^{10} to 1×10^{11} molecule cm^{-3}. Initial concentrations of O_3 and O_2 were 5×10^{13} and 1×10^{16} molecule cm^{-3}, respectively, from estimated concentrations within the experimental system. NO was subsequently added to the system at a concentration of 4.2×10^{14} molecule cm^{-3}. The resultant contour plot calculated using these input values is shown in Figure 4.

In this case, the calculated deviations are small over the range of experimental reagent concentrations used ($[HO_2] = (4-5) \times 10^{10}$ molecule cm^{-3} and $[ClO] = 5 \times 10^{11}$ to 6×10^{12} molecule cm^{-3}). At low [ClO], the deviation can be seen to be as much as 15%, although numerically for $[ClO] = 5 \times 10^{11}$ molecule cm^{-3} this would correspond to a change in k_3' of 2.8−3.2 s^{-1}; a difference certainly within the bounds of our experimental accuracy. The simulation suggests that for this combination of precursor molecules and initial reagent conditions, secondary reactions do not play a significant role. Furthermore, the titration process itself remains relatively unaffected by competing loss processes for Cl or ClO radicals. Consequently, no corrections were made to the experimentally determined values.

Excess ClO from Cl + Cl_2O, HO_2 from H + O_2 + M. Input concentrations of ClO were in the range of 5×10^{11} to 8×10^{12} molecule cm^{-3}; concentrations of initial HO_2 were in the range of 1×10^{10} to 1×10^{11} molecule cm^{-3}. Initial concentrations of Cl_2O and O_2 were also included at the outset of the model run with input values of 6×10^{12} and 1×10^{16} molecule cm^{-3}, respectively, obtained from estimates of the concentrations within the experimental system. NO was subsequently added to the system at a concentration of 2×10^{14} molecule cm^{-3}. The resultant contour plot calculated using these input values is shown in Figure 5.

As with the previous case, the simulations presented in Figure 5 suggest that the predicted deviations should be small for the initial experimental reagent and precursor molecule concentrations ($[ClO] = 3.5 \times 10^{11}$ to 9.5×10^{12} molecule cm^{-3}, $[HO_2] = (4-5) \times 10^{10}$ molecule cm^{-3}). For example, the predicted deviation if we have $[ClO] = 1 \times 10^{12}$ molecule cm^{-3} is approximately 12%. This corresponds to a change in k_3' from 5.7 to 6.3 s^{-1}. For $[ClO] = 7 \times 10^{12}$ molecule cm^{-3}, a −6% deviation is predicted. This corresponds to a change in k_3' from 39.6 to 37.2 s^{-1}. As a result, no corrections were made to the experimentally determined values for this combination of precursor molecules.

Excess ClO from O_3, HO_2 from F + H_2O_2. Input concentrations of ClO were in the range of 3×10^{11} to 5×10^{12} molecule cm^{-3}; concentrations of initial HO_2 were in the range of 1×10^{10} to 2×10^{11} molecule cm^{-3}. Initial concentrations of H_2O_2, O_3, and O_2 were 4×10^{12}, 2.5×10^{13}, and 8×10^{14} molecule cm^{-3}, respectively. NO was subsequently added to the system at a concentration of 2×10^{14} molecule cm^{-3}. The resultant contour plot calculated using these input values is shown in Figure 6.

Figure 6 shows that for the experimental conditions used ($[ClO] = 1.3 \times 10^{11}$ to 5.4×10^{12} molecule cm^{-3} $[HO_2] = (9-10) \times 10^{10}$ molecule cm^{-3}), the predicted deviations should be small enough to be neglected although they are higher than observed for the other two excess ClO combinations. For example, with an initial $[ClO] = 5 \times 10^{11}$ molecule cm^{-3}, a 20% deviation is predicted. This corresponds to a change in k_3' from 2.8 to 3.4 s^{-1}. At the other extreme, for a $[ClO] = 4 \times 10^{12}$ molecule cm^{-3} a −10% deviation is predicted by the model. This corresponds to a change in k_3' from 22.6 to 20.3 s^{-1}. Consequently, no corrections were made to these experimental results.

Comparison with Earlier Room-Temperature Data. The rate coefficient for the HO_2 + ClO reaction has been the subject of four earlier experimental studies at room temperature[8−11] and has been measured over a range of temperatures including room temperature in three studies.[12−14] The room-temperature results range from $(3.8-8.3) \times 10^{-12}$ cm^3 $molecule^{-1}$ s^{-1} and can be

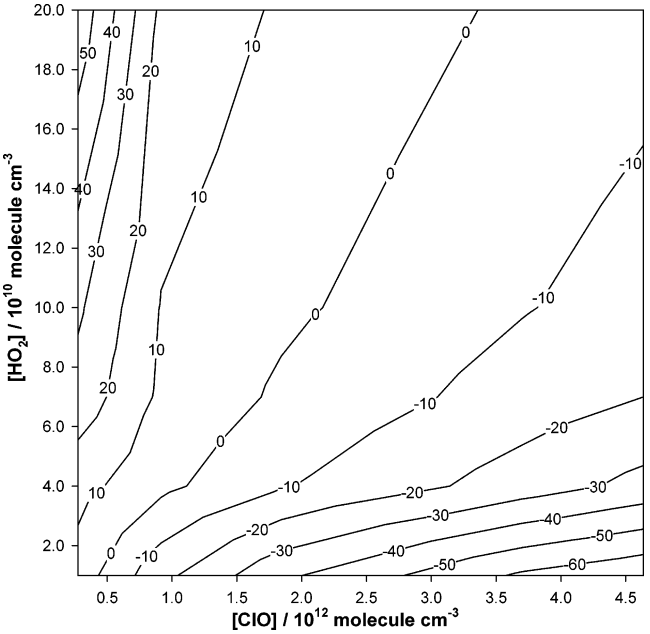

Figure 6. Calculated percent change in k_3' induced by secondary reactions and/or the titration process for a range of HO_2 and ClO concentrations from the precursor combination F + H_2O_2/Cl + O_3 with ClO as the excess reagent. Typical $[HO_2] = 1 \times 10^{11}$ molecule cm^{-3}. Percentage value reflects the difference between output and input values as given by del % = $((k_{3(out)}' - k_{3(in)}')/k_{3(in)}') \times 100$.

categorized as having been taken at either low (<10 Torr) or high (>50 Torr) pressures. The low-pressure data comprise four previous studies all of which used the flow tube technique. The first, by Reimann and Kaufman[8] used laser-induced fluorescence to detect HO_2 by first converting $HO_2 \rightarrow$ OH via reaction 8 as in this study. The kinetics of HO_2 decay in the presence of an excess of ClO formed by reaction 2 were subsequently followed. ClO concentrations were calculated from an extrapolation to the axis of the Cl atom resonance-fluorescence signal in the presence of varying ozone concentrations such that the [ClO] was taken to be the $[O_3]$ at the point where no Cl atom signal could be observed. k_3 was determined to be $(3.8 \pm 0.5) \times 10^{-12}$ cm^3 $molecule^{-1}$ s^{-1}. Leck et al.[9] coupled the flow tube technique with mass spectrometric detection of the HOCl product to monitor the kinetics of the reaction. ClO formed through reaction 2 was used as the excess reagent, and HO_2 was produced using reaction 6 and also through the reaction[7]

$$Cl + H_2O_2 \rightarrow HCl + HO_2 \qquad (30)$$

$$k_{30}(298\ K) = 4.1 \times 10^{-13}\ cm^3\ molecule^{-1}\ s^{-1}$$

ClO concentrations were determined by monitoring the Cl_2^+ ion signal with the microwave discharge switched on and off. The decrease in the ion signal at $m/e = 70$ upon activation of the discharge was taken to be proportional to the ClO concentration. k_3 was determined to be $(4.5 \pm 0.9) \times 10^{-12}$ cm^3 $molecule^{-1}$ s^{-1}. Stimpfle et al.[12] used laser magnetic resonance (LMR) detection to monitor both reactants. ClO was generated by reactions 2 and 15 and was held in excess over HO_2 which was produced via reaction 6. Decays of the HO_2 LMR signal in the presence of ClO were used to measure k_3. They determined $k_3 = (6.4 \pm 1.7) \times 10^{-12}$ cm^3 $molecule^{-1}$ s^{-1}. Knight et al.[14] coupled the flow tube technique with mass spectrometric detection. Seven different HO_2 and ClO precursor combinations were used to generate the reagents at room temperature, although ClO was held in excess for all experiments. The kinetics of the reaction were followed by observing the decay of the HO_2^+ signal at $m/e = 33$. A room-temperature value of $(7.1 \pm 0.9) \times 10^{-12}$ cm^3 $molecule^{-1}$ s^{-1} was measured for k_3 although it should be noted that these authors excluded data measured when using O_3 as a precursor for ClO formation via reaction 2. They suggest that there may have been vibrationally excited ClO present in their system from this reaction and that this effect and the slightly varying conditions from experiment to experiment may have contributed to the observation of systematically higher values and scatter for this precursor.

From a combination of these previously determined values, the mean of the low-pressure room-temperature data is 5.5×10^{-12} cm^3 $molecule^{-1}$ s^{-1}, but following the inclusion of the room-temperature data obtained in this study with a value of $k_3(296\ K) = (6.4 \pm 1.6) \times 10^{-12}$ cm^3 $molecule^{-1}$ s^{-1} with 2σ error limits, the average of the low-pressure data is raised slightly to 5.6×10^{-12} cm^3 $molecule^{-1}$ s^{-1}.

The high-pressure data (>50 Torr) comprise three previous studies of the rate coefficient at room temperature. All of these determinations used the flash photolysis technique coupled with UV absorption to observe both of the reactants. The two earliest of these studies by Burrows and Cox[10] and by Cattell and Cox[11] were performed using essentially the same apparatus where the modulated output from fluorescent blacklamps were used as the radical initiation source. The decay/formation profiles of the observed reactants were subsequently fit using a numerical chemical model where the rate coefficient of reaction 3 was allowed to vary until the best fit to the experimental data was derived. Initially, Burrows and Cox[10] photolyzed precursor mixtures of $Cl_2-Cl_2O-H_2-O_2-N_2$, whereas Cattell and Cox[11] photolyzed mixtures of $Cl_2-H_2-O_2-N_2$ to produce the ClO and HO_2 radicals. The respective authors determined values for $k_3 = (5.\ 4_{-2}^{+4}) \times 10^{-12}$ and $(6.2 \pm 1.5) \times 10^{-12}$ cm^3 $molecule^{-1}$ s^{-1} at room temperature. The latest study of the three, by Nickolaisen et al.,[13] used a xenon flash lamp to initiate radical chemistry. The radicals were produced by photolyzing two separate precursor mixtures, namely, $F_2-H_2-O_2-Cl_2O$ in a quartz cell (λ > 200 nm) and $Cl_2-Cl_2O-CH_3OH-O_2$ in a Pyrex cell (λ > 300 nm). The radical concentrations were followed using transient absorption spectrometry via a xenon lamp optimized for λ > 250 nm and a deuterium lamp optimized for the 200−250 nm region. The resultant decay profiles were fit using a numerical model where four parameters were allowed to vary for both of the precursor systems. For the F_2 system, the fractional dissociation of F_2 and Cl_2O and the rate coefficients for the HO_2 self-reaction and the process under investigation were variable. For the Cl_2 system, the initial Cl concentration and the rate coefficients for the HO_2 self-reaction, the reaction of Cl with Cl_2O, and the process under investigation were allowed to vary. k_3 was then extracted from the best fit values. They determined values of $k_3 = (8.26 \pm 1.38) \times 10^{-12}$ and $(7.78 \pm 0.83) \times 10^{-12}$ cm^3 $molecule^{-1}$ s^{-1} for the F_2 and Cl_2 precursor systems, respectively, at room temperature.

The average of the high-pressure results at room temperature for k_3 is slightly larger, with a value of 6.5×10^{-12} cm^3 $molecule^{-1}$ s^{-1}. Although this difference suggests that there may be a pressure-dependent component to the total rate coefficient, systematic attempts to observe this dependence at room temperature have been unsuccessful.[11,13] The combined uncertainties of the high- and low-pressure data overlap, however. Two recent evaluations, specifically those of Sander et al.[6] and Atkinson et al.[32], recommend values of 5.6×10^{-12} and 6.9×10^{-12} cm^3 $molecule^{-1}$ s^{-1}, respectively. Our value of $(6.4 \pm 1.6) \times 10^{-12}$

cm^3 $molecule^{-1}$ s^{-1} lies between the two evaluations, but the experimental uncertainties in our data cover both of these recommended numbers.

Comparison with Earlier Temperature-Dependent Data. The three earlier temperature-dependent measurements of the rate coefficient for reaction 3 have significant differences among their findings. The earliest study by Stimpfle et al.[12] observed that there was a marked rise in the rate coefficient with falling temperature. Above 298 K their data was essentially temperature independent, but from 233−298 K a value for (Ea/*R*) = −709 K was found to best fit the derived data. They concluded from the unusual temperature dependence below room-temperature that two different mechanisms could be occurring, namely, reaction of ClO with HO_2 to form the HOOClO or HOOOCl cyclic collision complexes. In this way, the complex could either fall apart to the reactants or continue on to the products HOCl + O_2 or HCl + O_3, respectively. As they did not detect any products, however, they state that this was a hypothetical proposition and that it could also be possible that both collision complexes could fall apart to form the same products. They ascribed the rapidly increasing value of k_3 with falling temperature to the formation of a collisional complex with less internal energy such that the probability of it proceeding to products rather that falling apart to reactants was enhanced at low temperatures. They cite a negative non-Arrhenius expression for $k_3 = 3.3 \times 10^{-11} \exp(-850/T) + 4.5 \times 10^{-12} (T/300)^{-3.7}$ cm^3 $molecule^{-1}$ s^{-1}. In contrast, Nickolaisen et al.[13] determined a temperature dependence for k_3 which displayed a less pronounced negative Arrhenius behavior over their entire temperature range of 203−364 K although the values for the rate coefficients themselves were systematically higher than those determined by earlier studies. They cite an expression for $k_3 = 2.84 \times 10^{-12} \exp\{(312 \pm 60)/T\}$ cm^3 $molecule^{-1}$ s^{-1}. The final study of the temperature dependence of the ClO + HO_2 reaction by Knight et al.[14] in contrast to the other two concluded that only a weakly positive temperature dependence exists. They suggest an expression for $k_3 = (7.1 \pm 0.4) \times 10^{-12} \exp\{(-16 \pm 17)/T\}$ cm^3 $molecule^{-1}$ s^{-1} but considering the overall uncertainties in their measurements cite a final temperature-independent value for $k_3 = (7.1 \pm 1.8) \times 10^{-12}$ cm^3 $molecule^{-1}$ s^{-1}.

The present study has added to the currently available temperature-dependent data on the rate coefficient for the ClO + HO_2 reaction and in common with the Nickolaisen et al.[13] study determines a negative Arrhenius expression for $k_3 = (1.75 \pm 0.52) \times 10^{-12} \exp[(368 \pm 78)/T]$ cm^3 $molecule^{-1}$ s^{-1}. The (Ea/*R*) factors derived by these two studies are in good agreement although the pre-exponential factors are outside of the combined uncertainties. Current evaluations of the same quantities by the NASA data panel[6] and by the IUPAC evaluation[32] give $k_3 = 2.7 \times 10^{-12} \exp(220/T)$ and $2.2 \times 10^{-12} \exp(340/T)$ cm^3 $molecule^{-1}$ s^{-1}, respectively. The basis of the current NASA evaluation[6] for k_3 Arrhenius parameters includes the results from an unpublished study[33] and should therefore be used with caution. The latest IUPAC[32] evaluation derives a value for (Ea/*R*) from an average of those obtained by the three earlier temperature-dependent studies using the $T < 298$ K value of −709 K for (Ea/*R*) by Stimpfle et al.[12] It can be seen that the agreement between this study and the current IUPAC[32]-derived parameters is reasonably good although our determination of the pre-exponential factor is somewhat lower but still within the experimental uncertainty.

Theoretical Considerations. The body of theoretical work on the ClO−HO_2 system consists of 10 earlier studies which range from calculations of the transition states and likely reaction pathways to predictions of the rate coefficient. As an aside to their experimental work, Stimpfle et al.[12] performed simple group additivity calculations on the HO_2 + ClO reaction and concluded that the dissociation energy of one potential intermediate, HOOOCl, was probably too small for it to be stable. Mozurkewich[15] performed RRKM calculations to determine the possible intermediates of reaction 3. He hypothesized that three intermediates were likely to form, namely, OClOOH, HOOOCl, and a hydrogen-bonded intermediate O_2H−OCl. He hypothesized that all three of these species should be weakly bound and therefore have little or no pressure dependence. Furthermore, he suggested that the binding energies involved would be insufficient to allow a cyclic transition state to form such that direct hydrogen abstraction was the most likely reaction mechanism. Toohey and Anderson[16] using Hartree−Fock and Møller−Plesset molecular orbital methods calculated that two different reaction mechanisms should be occurring. They suggested that at high temperatures reaction 3 should proceed through a H atom abstraction by ClO from HO_2. At lower temperatures, the mechanism was calculated to involve a covalently bound OClOOH cyclic intermediate which would eliminate HOCl and O_2. Buttar and Hirst[17] also using similar ab initio methods calculated that the reaction could proceed exothermically on the singlet surface in addition to the triplet surface. In common with Mozurkewich[15] and Toohey and Anderson,[16] they proposed that a direct H atom abstraction mechanism on the triplet surface should dominate at higher temperatures, but reaction on the singlet energy surface involving the possibility of a relatively long-lived HOOOCl intermediate could play a role at lower temperatures through a 1,2 H atom shift to form HOCl + O_2. McGrath et al.[18] and Rohlfing[19] used ab initio molecular orbital methods to calculate geometries and energies of the possible $HClO_3$ intermediates. Rohlfing[19] determined that $HOClO_2$ would be the most stable isomer. Francisco and Sander[20] improved on these two studies by calculating the likely positions of various spectral features of the $HClO_3$ singlet isomers such that these species might be identified in addition to determining the energy ordering of these intermediates. Furthermore, these authors suggested that the most stable isomer, $HOClO_2$, might be long-lived enough to act as a temporary reservoir for inorganic chlorine in the lower stratosphere. Phillips and Quelch[21] used MCSCF ab initio methods to calculate the energy of the HOOOCl intermediate. They concluded that the 16 kcal/mol binding energy, in contrast to the 2 kcal/mol estimate of Stimpfle et al.,[12] was sufficient for the molecule to be of potential importance under stratospheric conditions. Nickolaisen et al.[13] provided complementary information to their experimental study by undertaking an ab initio study of the potential surface for the HO_2 + ClO reaction. They concluded that HOOOCl and HOOClO formation was facile; however, large energy barriers on the singlet surface would hinder the formation of products from these intermediates. Additionally, in common with earlier theoretical studies they suggested that reaction takes place primarily over the triplet surface through a hydrogen-bonded intermediate and that if formed in the lower stratosphere, HOOOCl might be readily photolyzed to produce either HO_2 + ClO or ClOO + OH. Consequently, the second set of products would influence O_3 concentrations in this region, or alternatively, HOOOCl may also react with other radical species. More recently, Kaltsoyannis and Rowley[22] in good agreement with Nickolaisen et al.[13] also

calculated that reaction 3 would proceed primarily on the triplet surface and that the barrier for HOOOCl dissociation to $HCl + O_3$ of 90 kJ/mol would essentially leave the branching ratio for reaction channel 3b at zero. Their calculation of an (Ea/*R*) value $= -960$ K suggests a larger negative temperature dependence than is experimentally observed and it is also significantly larger than expected from current evaluations.[6,32] They concluded, in common with other studies, that HOOOCl should be thermally stable and therefore may play a role in atmospheric halogen chemistry. Finally, the most recent study by Xu et al.[23] has attempted a theoretical prediction for k_3 using ab initio molecular orbital methods. In this work, they suggest that the formation of two HOOOCl isomers over the singlet surface contributes significantly to the observed rate coefficient. As before, they conclude that the dominant mechanism for reaction occurs through the triplet surface via a O_2H-OCl hydrogen-bonded complex. However, they hypothesize that below room temperature, k_3 should be seen to be increasingly influenced by the stabilization of HOOOCl at higher pressures. At low pressures, they suggest that the rate should be dominated by the abstraction process. At all pressures, formation of $HCl + O_3$, $HOCl + {}^1O_2$ and $OH + ClOO/OClO$ should be unimportant due to the high-energy barriers although HOOOCl formation should occur readily at pressures >1 Torr. They predicted the total rate coefficient at 1, 400, and 760 Torr pressures to reflect the currently available experimental data. The respective curves are plotted in Figure 2 alongside the current experimentally determined values. It can be seen that the theoretical predictions by Xu et al.[23] somewhat resolve the differences between the temperature-dependent high- and low-pressure data as being largely due to the formation and subsequent collisional stabilization of the HOOOCl intermediate. The high-pressure curves agree well with the data from Nickolaisen et al.[13] below room temperature, whereas the prediction for 1 Torr shows reasonable agreement with the Knight et al.[14] values and excellent agreement with the current study. The low-temperature Stimpfle et al.[12] data remain anomalous, however, and no nonlinear Arrhenius behavior has been observed in the present work or in any of the earlier temperature-dependent studies.

The general consensus among the theoretical work indicates that the dominant reaction mechanism is that of a direct H atom abstraction from HO_2 by ClO on the triplet energy surface to form $HOCl + {}^3O_2$. Furthermore, at low temperatures, formation of HOOOCl and HOOClO should be facile over the singlet energy surface although the barriers to formation of the minor products $HOCl + {}^1O_2$, $HCl + O_3$, and $OH + ClOO/OClO$ are prohibitively large. This hypothesis is supported by the lack of experimental evidence to date for the formation of any products other than $HOCl + O_2$ in the gas phase.[9,10,14,34] The only study to date to observe alternative products for reaction 3 by Finkbeiner et al.[35] used the matrix isolation technique coupled with FTIR spectroscopy. They observed a small production of O_3 less than or equal to 5% of the total product formation. Collisional stabilization of the isomers of $HClO_3$ at low temperatures as they are formed with less internal excitation could mean that significant concentrations of these species might be produced and at least one of the $HClO_3$ isomers could have an appreciable lifetime in the stratosphere. Further work is required to isolate these species at lower temperatures to determine their possible photochemistry and their potential reactivity with other reactive species. Moreover, the hypothesis of Xu et al.[23] suggests that supplemental theoretical and experimental studies are needed to elucidate the pressure dependence of the $HO_2 + ClO$ reaction at temperatures lower than 298 K.

Acknowledgment. The research described in this article was performed at the Jet Propulsion Laboratory, California Institute of Technology under a contract with the National Aeronautics and Space Administration and was supported by the NASA Upper Atmosphere Research and Tropospheric Chemistry Programs. Technical support from D. Natzic is gratefully acknowledged.

References and Notes

(1) Clerbaux, C.; Cunnold, D.M. et al. Long-Lived Compounds. In *Scientific Assessment of Ozone Depletion: 2006*; Global Ozone and Monitoring Research Project−Report No. 50; World Meteorological Organization: Geneva, Switzerland, 2007; Chapter 1.

(2) (a) Butler, J. H.; Battle, M.; Bender, M. L.; Montzka, S. A.; Clarke, A. D.; Saltzman, E. S.; Sucher, C. M.; Severinghaus, J. P.; Elkins, J. W. *Nature* **1999**, *399*, 749. (b) Sturrock, G. A.; Etheridge, D. M.; Trudinger, C. M.; Fraser, P. J.; Smith, A. M. *J. Geophys. Res., [Atmos.]* **2002**, *107*, 4765. (c) Kaspers, K. A.; van de Wal, R. S. W.; de Gouw, J. A.; Hofstede, C. M.; van den Broeke, M. R.; van der Veen, C.; Neubert, R. E. M.; Meijer, H. A. J.; Brenninkmeijer, C. A. M.; Karlof, L.; Winther, J. G. *J. Geophys. Res., [Atmos.]* **2004**, *109*, D02307, doi:10.1029/2003JD003950. (d) McCulloch, A. *Chemosphere* **2002**, *47*, 667. (e) Trudinger, C. M.; Etheridge, D. M.; Sturrock, G. A.; Fraser, P. J.; Krummel, P. B.; McCulloch, A. *J. Geophys. Res., [Atmos.]* **2004**, *109*, D22310, doi:10.1029/2004JD004932.

(3) Farman, J. C.; Gardiner, B. G.; Shanklin, J. D. *Nature* **1985**, *315*, 207.

(4) Fioletov, V. E.; Bodeker, G. E.; Miller, A. J.; McPeters, R. D.; Stolarski, R. *J. Geophys. Res., [Atmos.]* **2002**, *107*, 4647.

(5) Solomon, S.; Garcia, R. R.; Rowland, F. S.; Wuebbles, D. J. *Nature* **1986**, *321*, 755.

(6) Sander, S. P.; Finlayson-Pitts, B. J.; Friedl, R. R.; Golden, D. M.; Huie, R. E.; Keller-Rudek, H.; Kolb, C. E.; Kurylo, M. J.; Molina, M. J.; Moortgat, G. K.; Orkin, V. L.; Ravishankara, A. R.; Wine, P. H. *Chemical Kinetics and Photochemical Data for Use in Atmospheric Studies, Evaluation No. 15*; JPL Publication 06-2; Jet Propulsion Laboratory: Pasadena, CA, 2006. http://jpldataeval.jpl.nasa.gov/.

(7) Wennberg, P. O.; Cohen, R. C.; Stimpfle, R. M.; Koplow, J. P.; Anderson, J. G.; Salawitch, R. J.; Fahey, D. W.; Woodbridge, E. L.; Keim, E. R.; Gao, R. S.; Webster, C. R.; May, R. D.; Toohey, D. W.; Avallone, L. M.; Proffitt, M. H.; Loewenstein, M.; Podolske, J. R.; Chan, K. R.; Wofsy, S. C. *Science* **1994**, *266*, 398.

(8) Reimann, B.; Kaufman, F. *J. Chem. Phys.* **1978**, *69*, 2925.

(9) Leck, T. J.; Cook, J. E. L.; Birks, J. W. *J. Chem. Phys.* **1980**, *72*, 2364.

(10) Burrows, J. P.; Cox, R. A. *J. Chem. Soc., Faraday Trans. 1* **1981**, *77*, 2465.

(11) Cattell, F. C.; Cox, R. A. *J. Chem. Soc., Faraday Trans. 2* **1986**, *82*, 1413.

(12) Stimpfle, R. M.; Perry, R. A.; Howard, C. J. *J. Chem. Phys.* **1979**, *71*, 5183.

(13) Nickolaisen, S. L.; Roehl, C. M.; Blakeley, L. K.; Friedl, R. R.; Francisco, J. S.; Liu, R. F.; Sander, S. P. *J. Phys. Chem. A* **2000**, *104*, 308.

(14) Knight, G. P.; Beiderhase, T.; Helleis, F.; Moortgat, G. K.; Crowley, J. N. *J. Phys. Chem. A* **2000**, *104*, 1674.

(15) Mozurkewich, M. *J. Phys. Chem.* **1986**, *90*, 2216.

(16) Toohey, D. W.; Anderson, J. G. *J. Phys. Chem.* **1989**, *93*, 1049.

(17) Buttar, D.; Hirst, D. M. *J. Chem. Soc., Faraday Trans.* **1994**, *90*, 1811.

(18) McGrath, M. P.; Clemitshaw, K. C.; Rowland, F. S.; Hehre, W. J. *J. Phys. Chem.* **1990**, *94*, 6126.

(19) Rohlfing, C. M. *Chem. Phys. Lett.* **1995**, *245*, 665.

(20) Francisco, J. S.; Sander, S. P. *J. Phys. Chem.* **1996**, *100*, 573.

(21) Phillips, D. H.; Quelch, G. E. *J. Phys. Chem.* **1996**, *100*, 11270.

(22) Kaltsoyannis, N.; Rowley, D. M. *Phys. Chem. Chem. Phys.* **2002**, *4*, 419.

(23) Xu, Z. F.; Zhu, R. S.; Lin, M. C. *J. Phys. Chem. A* **2003**, *107*, 3841.

(24) Hickson, K. M.; Keyser, L. F. *J. Phys. Chem. A* **2005**, *109*, 6887.

(25) Kurylo, M. J. *J. Phys. Chem.* **1972**, *76*, 3518.

(26) Anderson, J. G.; Margitan, J. J.; Kaufman, F. *J. Chem. Phys.* **1974**, *60*, 3310.

(27) Mallard, W. G.; Westley, F.; Herron, J. T.; Hampson, R. F.; Frizzell, D. H. *NIST Chemical Kinetics Standard Reference Database 17*, version 7.0 (Web version), release 1.2. http://kinetics.nist.gov/; National Institute of Standards and Technology: Gaithersburg, MD, 2007.

(28) Poulet, G.; Laverdet, G.; Lebras, G. *J. Phys. Chem.* **1986**, *90*, 159.
(29) Lee, Y. P.; Stimpfle, R. M.; Perry, R. A.; Mucha, J. A.; Evenson, K. M.; Jennings, D. A.; Howard, C. J. *Int. J. Chem. Kinet.* **1982**, *14*, 711.
(30) Marrero, T. R.; Mason, E. A. *J. Phys. Chem. Ref. Data* **1972**, *1*, 3.
(31) Wang, J. J.; Keyser, L. F. *J. Phys. Chem. A* **1999**, *103*, 7460.
(32) Atkinson, R.; Baulch, D. L.; Cox, R. A.; Crowley, J. N.; Hampson, R. F., Jr.; Hynes, R. G.; Jenkin, M. E.; Kerr, J. A.; Rossi, M. J.; Troe, J. *IUPAC Subcommittee on Gas Kinetic Data Evaluation for Atmospheric Chemistry*, Web version; February 2006. http://www.iupac-kinetic.ch.cam.ac.uk/; adapted from *Atmos. Chem. Phys. Discuss.* **2006**, *6*, 2281.
(33) Laszlo, B.; Friedl, R. R.; Sander, S. P. Cited in ref 6.
(34) Leu, M. T. *Geophys. Res. Lett.* **1980**, *7*, 173.
(35) Finkbeiner, M.; Crowley, J. N.; Horie, O.; Muller, R.; Moortgat, G. K. *J. Phys. Chem.* **1995**, *99*, 16264.